Article ID: 1000-7032(2018)08-1087-08

Synthesis and Luminescence of α-$Ba_3Y(BO_3)_3:Dy^{3+}$ Phosphors

NING Hong-yu, CHENG Zhi-yuan, DONG Chao,
HU Ze-qing, YU Jing-jie*, ZHANG Yan-jie*

(*Research Institute of Photonics, Dalian Polytechnic University, Dalian* 116034, *China*)

* *Corresponding Authors, E-mail: yujingjie@ dlpu. edu. cn; zhang_yj@ dlpu. edu. cn*

Abstract: A series of phosphors α-$Ba_3Y(BO_3)_3:Dy^{3+}$ have been synthesized *via* conventional solid-state method and characterized. Fluorescence spectra (FL) show that the as-synthesized phosphors mainly exhibit two dominating emission peaks at 488 and 577 nm corresponding to the transitions from $^4F_{9/2}$ to $^6H_{15/2}$ and $^6H_{13/2}$, respectively under ultraviolet (UV) or blue radiation. The best synthesis temperature is 1 100 ℃, leading to the most intensive luminescence, pure phase and most sufficient crystal growth ensured by FL, X-ray diffraction (XRD) and scanning electron microscope (SEM), respectively. The concentration quenching mechanism has been determined to be mainly dipole-dipole interaction and exchange interaction is not negligible due to the specific unit cell structure; the critical concentration is 0.07. The second-order exponential lifetime decay curves are observed and its origin related to the specific unit cell structure is discussed. The as-synthesized phosphor has potential application for pc-WLEDs in the lighting field.

Key words: phosphors; α-$Ba_3Y(BO_3)_3:Dy^{3+}$; crystal structure

CLC number: O482.31 **Document code**: A **DOI**: 10.3788/fgxb20183908.1087

α-$Ba_3Y(BO_3)_3:Dy^{3+}$ 荧光粉的合成及其发光性能

宁宏宇, 程志远, 董 超, 胡泽青, 于晶杰*, 张彦杰*

(大连工业大学 光子学研究所, 辽宁 大连 116034)

摘要: 采用传统的固相法成功合成了一系列 α-$Ba_3Y(BO_3)_3:Dy^{3+}$ 荧光粉,使用 X 射线衍射(XRD)、扫描电镜(SEM)、荧光光谱(FL)和寿命衰减曲线等对样品进行表征。结果表明:在近紫外/蓝光激发下,样品的发射光谱主要包含黄(577 nm)、蓝(488 nm)两个发射峰组成,分别对应电子跃迁$^4F_{9/2}\rightarrow{}^6H_{13/2}$和$^4F_{9/2}\rightarrow{}^6H_{15/2}$。最佳合成温度为 1 100 ℃,该条件下合成的样品具有纯相、最大结晶度和最大发光强度。研究了荧光粉的浓度猝灭效应,猝灭机理主要是 dipole-dipole interaction,同时 exchange interaction 无法忽略,临界摩尔分数为0.07。样品的寿命衰减曲线为二次指数型,这与 $Ba_3Y(BO_3)_3$ 特有的晶格结构有直接关系。α-$Ba_3Y(BO_3)_3:Dy^{3+}$ 荧光粉有应用于荧光转换型白光 LED 照明的潜力。

关 键 词: 荧光粉; α-$Ba_3Y(BO_3)_3:Dy^{3+}$; 晶格结构

收稿日期: 2017-12-11; **修订日期**: 2018-01-25

基金项目: 辽宁省自然科学基金(20170540074)资助项目
Supported by Natural Science Foundation of Liaoning Province(20170540074)

1 Introduction

In lighting field, phosphor converted white light emitting diodes (pc-WLEDs) play an important role as solid-state light (SSL) due to their outstanding performances, such as high efficiency, energy saving, long lifetime and environment friendly. To obtain whitle light, LED chip must be coated with tricolor phosphors or white light emitting single matrix phosphors. While the development of the blue and ultraviolet (UV) chips, lots of contributions are focused on novel phosphors for LED chips[1-2], especially blue, green, red and white phosphors.

Many kinds of mineral salts could be used as host material, such as tungstates, vanadates, aluminates, phosphates, borates and silicates[3-9]. Because of the low synthesis temperature, stable physical chemical property and various crystal structures of borates, theses concentrating on rare earth (RE) ions doped borate phosphor are reported very frequently[9-16]. Among all sorts of borates, α-$Ba_3Y(BO_3)_3$ with layered crystal structure belonging to hexagonal system has been proved to be qualified matrix for Eu^{3+}, Ce^{3+} and Tb^{3+} activated phosphor with single colour luminescence[17-18]. As far as we know, luminescence properties of Dy^{3+} doped α-$Ba_3Y(BO_3)_3$ phosphor haven't been reported yet. Trivalent dysprosium is very promising because its emission spectrum consists of two peaks at blue and yellow region, corresponding to electronic transition from $^4F_{9/2}$ to $^6H_{15/2}$ and $^6H_{13/2}$, respectively. Therefore, doping in proper matrix, Dy^{3+} ions could emit white light without co-doping any other activators[19-21]. It's significant to scope the luminescence behavior of Dy^{3+} doped α-$Ba_3Y(BO_3)_3$.

In this work, α-$Ba_3Y(BO_3)_3$: Dy^{3+} phosphors were synthesized at different temperature by traditional solid state method. Crystal structure, morphology, luminescence and lifetime properties were explored. The concentration quenching mechanism was supposed to be relative to the unique crystal structure.

2 Experiments

The α-$Ba_3Y_{1-x}(BO_3)_3$: xDy^{3+} phosphors were prepared *via* a conventional solid state method using Dy_2O_3 (99.99%), $BaCO_3$ (A.R.), Y_2O_3 (99.99%) and H_3BO_3 (A.R.) as starting materials without any further purification. All materials were weighed stoichiometrically except H_3BO_3 with 3% (mass fraction) overdose for charge compensation; mixed and ground thoroughly in an agate mortar for 30 min. Then the homogeneous mixture was transferred to a corundum crucible, heated at 170 ℃ for 60 min in furnace. After cooled down with the furnace, samples were ground and mixed again, heated at 850, 1 000, 1 100 ℃ for 400 min in atmosphere. Finally, the crystalline powders were obtained.

The phases were identified by XRD (XRD-7000S, Shimadzu, 40 kV and 30 mA, Cu Kα, λ = 0.154 056 nm, 0.02° by step); the morphology was photographed by a SEM (JSM7800F, JOEL); the luminescence spectra were recorded by a HITACH F-4500 fluorescence spectrophotometer with a xenon lamp operated at room temperature; the lifetime decay curves (λ_{ex} = 350 nm, λ_{em} = 577 nm) were investigated using a spectrofluorometer (HJY, TRIAX550) with a laser source (Horizon, OPO system, 10 Hz).

3 Results and Discussion

3.1 XRD and Morphology

α-$Ba_3Y(BO_3)_3$ has a hexagonal layered structure with space group $P63cm$(185) and unit cell parameters $a = b = 0.941\ 9$ nm, $c = 1.759\ 5$ nm, $V = 1.351\ 87$ nm^3 and $Z = 6$. As shown in Fig. 1, there are 4 and 2 lattice sites for Ba^{2+} and Y^{3+} ions, respectively, separated by paralleled planes formed by BO_3^{3-} anion groups. Basically, this unusual structure can be described as multilayer sandwiches: BO_3^{3-} anion groups are bread and cations are fillings. All Y^{3+} ions are arranged in the same layers named as Y, then the left layer of BO_3^{3-} to Y can be named as 'bread A' and the right one as 'bread B'. The layer of BO_3^{3-} separating Ba1 and Ba2 can be named as 'bread C'. Ba1/Ba3 sites are set between C and A while Ba2 and Ba4 sites between B and C, respectively. Meanwhile, Ba3/Ba4 are much closer to the nearest Y sites with

distance about 0.387 6/0.390 9 nm than Ba1/Ba2 sites[22].

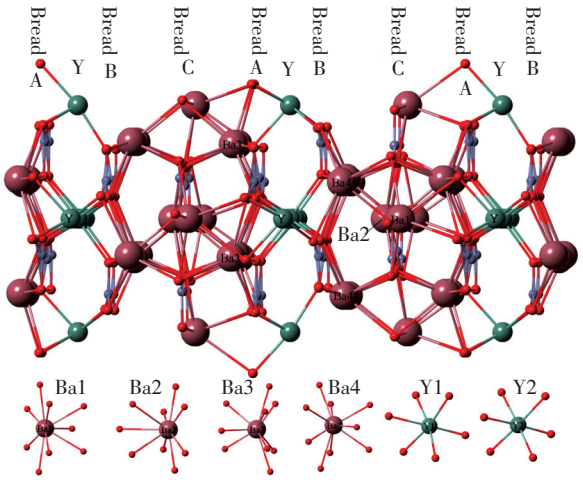

Fig. 1　Unit cell structure of α-$Ba_3Y(BO_3)_3$ and the coordination environment of Y^{3+} and Ba^{2+} ions in the host lattice

Fig. 2 presents the normalized XRD patterns of α-$Ba_3Y_{0.93}(BO_3)_3$:0.07Dy^{3+} synthesized at 850, 1 000, 1 100 ℃, respectively and the standard of α-$Ba_3Y(BO_3)_3$ (PDF No. 51-1849). Compared with the standard patterns, sample synthesized at 850 ℃ mainly belongs to α-$Ba_3Y(BO_3)_3$ phase and the weak impurity belongs to YBO_3 marked by ▼. However, samples synthesized at 1 000 and 1 100 ℃ only show peaks of α-$Ba_3Y(BO_3)_3$ without any significant impurity, indicating that pure phase of α-$Ba_3Y(BO_3)_3$ has been achieved.

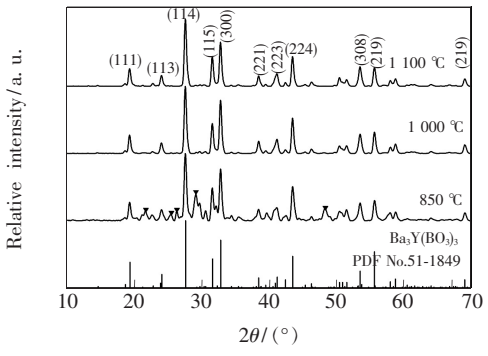

Fig. 2　XRD patterns of α-$Ba_3Y_{0.93}(BO_3)_3$:0.07Dy^{3+} synthesized at 1 100, 1 000, 850 ℃, respectively and the standard of α-$Ba_3Y(BO_3)_3$ (PDF No. 51-1849).

Fig. 3 presents the XRD patterns of α-$Ba_3Y_{1-x}(BO_3)_3$:xDy^{3+} (x = 0.00, 0.03, 0.07, 0.05, 0.09, 0.12, 0.15, respectively) synthesized at 1 100 ℃ and the standard. XRD patterns of all samples have the same discipline and accord with the standard, suggesting that substituting with Dy^{3+} ions barely affects the crystal structure. No significant offset of diffraction peak is observed, which can be explained by the low doping concentration of Dy^{3+} and the tiny difference between the radius of Dy^{3+} and Y^{3+} (0.091 2 nm for Dy^{3+} and 0.090 nm for Y^{3+}).

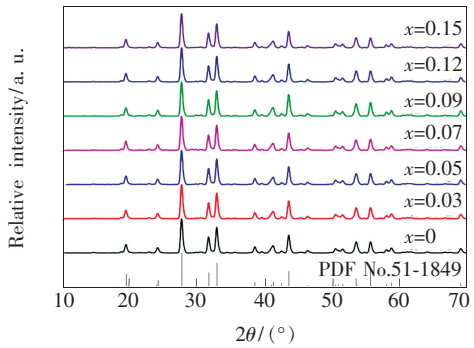

Fig. 3　XRD patterns of α-$Ba_3Y_{1-x}(BO_3)_3$:xDy^{3+} synthesized at 1 100 ℃ and the standard of α-$Ba_3Y(BO_3)_3$ (PDF No. 51-1849)

Fig. 4 exhibits the morphology of α-$Ba_3Y_{0.93}(BO_3)_3$:0.07Dy^{3+} synthesized at 850, 1 000, 1 100 ℃, respectively and α-$Ba_3Y(BO_3)_3$ synthesized at 1 100 ℃. When synthesized at 850 ℃, phosphor consists of many small particles without certain shape and much less number of bigger layered particles. As mentioned before, α-$Ba_3Y(BO_3)_3$ has a layered structure, similar with the layered particles, and XRD proves that sample basically has α-$Ba_3Y(BO_3)_3$ phase with some impurity, thus one can conclude that the layered particles have the isostructure with α-$Ba_3Y(BO_3)_3$. When synthesized at 1 000 and 1 100 ℃, only layered particles with even bigger size and fragments generated from grinding are found, suggesting that pure phase of α-$Ba_3Y(BO_3)_3$ with no impurity achieved, fitting with the XRD result. Based on the particle size and appearance, when synthesized at 1 100 ℃, the degree of crystal growth is the most sufficient; in another word, 1 100 ℃ is the best synthesis temperature for α-$Ba_3Y(BO_3)_3$. Further more, the particle size and appearance of α-$Ba_3Y_{0.93}(BO_3)_3$:0.07Dy^{3+} and α-$Ba_3Y(BO_3)_3$ obtained at 1 100 ℃ don't differ much from each other, indicating that substituting with Dy^{3+} ions doesn't influence the morphology, either.

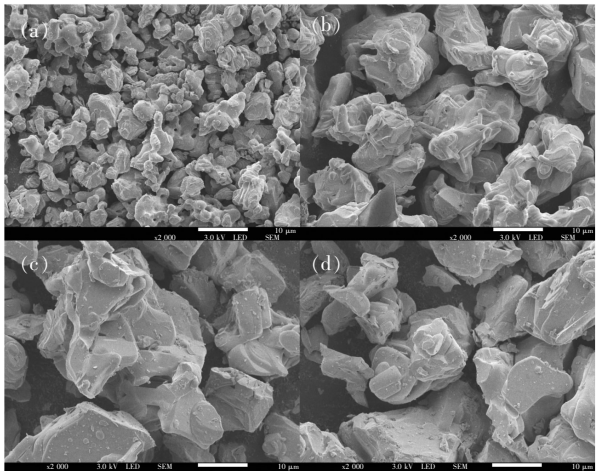

Fig. 4 Morphology of α-$Ba_3Y_{0.93}(BO_3)_3$:0.07Dy^{3+} synthesized at 850 ℃(a), 1 000 ℃(b), 1 100 ℃(c) and α-$Ba_3Y(BO_3)_3$ synthesized at 1 100 ℃(d).

3.2 Luminescence of α-$Ba_3Y(BO_3)_3$:Dy^{3+}

Fig. 5 illustrates the excitation and emission spectra of sample α-$Ba_3Y(BO_3)_3$:Dy^{3+} monitored at 488 and 350 nm, respectively. In the UV and blue region, a series of peaks at 326, 350, 365, 387, 425, 454 nm corresponding to electron transitions within $4f^9$ configuration from the ground state $^6H_{15/2}$ to $^7F_{5/2}$, $^4M_{15/2}+{}^6P_{5/2}$, $^4I_{11/2}+{}^6P_{7/2}$, $^4I_{13/2}+{}^4F_{7/2}$, $^4G_{11/2}$ and $^4I_{15/2}$ are observed in the excitation spectrum, among which transition $^6H_{15/2}\rightarrow{}^4M_{15/2}$ ($^6P_{5/2}$) at 350 nm dominates. Meanwhile, the emission spectrum ($\lambda_{ex}=350$ nm) mainly consists of two peaks at 488 nm due to a forced magnetic dipole transition $^4F_{9/2}\rightarrow{}^6H_{15/2}$ and 577 nm due to a hypersensitive forced electric dipole transition $^4F_{9/2}\rightarrow{}^6H_{13/2}$ strongly influenced by the doping environment, respectively. Generally, when Dy^{3+} occupies a high symmetry lattice site with an inverse centre, the yellow emission is weaker than the other; otherwise it exceeds. In our case, transition $^4F_{9/2}\rightarrow{}^6H_{15/2}$ surpasses $^4F_{9/2}\rightarrow{}^6H_{13/2}$, indicating that Dy^{3+} ions tend to occupy centrosymmetrical sites, namely Y sites according to Fig. 1. In summary, Dy^{3+} doped α-$Ba_3Y(BO_3)_3$ could be excited by UV and blue light (namely, 350 nm and 454 nm) effectively and emit white light, promising a potential application for pc-WLEDs in the outdoor lighting and display fields.

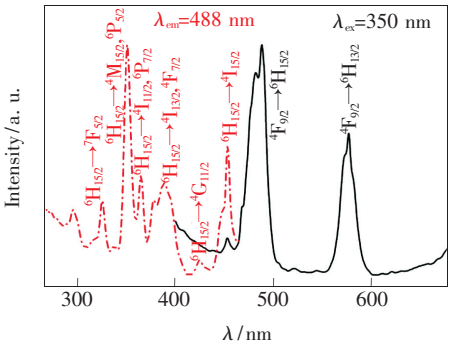

Fig. 5 Excitation (left) and emission (right) spectra of α-$Ba_3Y(BO_3)_3$:Dy^{3+}

3.3 Influence of Synthesis Temperature and Doping Concentration of Dy^{3+}

The emission spectra of α-$Ba_3Y_{0.93}(BO_3)_3$:0.07Dy^{3+} synthesized at 1 100, 1 000 and 850 ℃ are presented in Fig. 6. As the synthesis temperature rising from 850 to 1 100 ℃, the luminescent intensity increases as well. It's been mentioned before that the degree of crystal growth can be strongly influenced by synthesis temperature, and samples grow most sufficiently at 1 100 ℃. The most intense

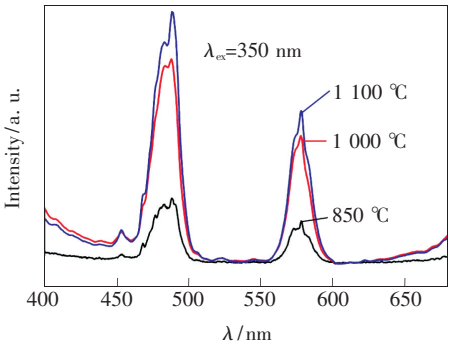

Fig. 6 Emission spectra of α-$Ba_3Y_{0.93}(BO_3)_3$:0.07Dy^{3+} synthesized at 1 100, 1 000 and 850 ℃, respectively.

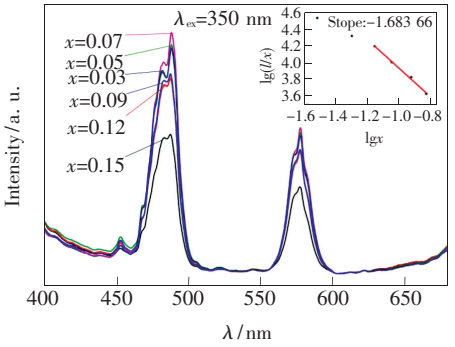

Fig. 7 Emission spectra of α-$Ba_3Y_{1-x}(BO_3)_3$:xDy^{3+}. The inset is the linear dependence of lg(I/x) on lg$x$.

luminescence shall be originated from the most sufficient crystal growth.

To invest the influence of Dy^{3+} concentration (x) on the luminescence behavior and obtain the best intensity, a series of α-$Ba_3Y_{1-x}(BO_3)_3$: xDy^{3+} ($x=0.03$, 0.05, 0.07, 0.09, 0.12, 0.15) are synthesized and their emission spectra are demonstrated in Fig. 7. The luminescent intensity first increases slowly while x increasing from 0.03 to 0.07, and then decreases rapidly if x increases persistently, hence $x=0.07$ is the optimum concentration (χ_c). There are lot of energy levels between $^6F_{1/2}$ and $^6H_{11/2}$ of Dy^{3+} and many ways of energy transfer between different Dy^{3+} ions to decrease the population of Dy^{3+} ions on the $^4F_{9/2}$ level without any photon emitted. The numerous cross relaxations are the main reason for the low critical concentration (χ_c) of Dy^{3+} [23]. Another interesting characteristic is the barely changeable yellow-to-blue intensity ratio (Y/B ratio) of Dy^{3+} ions varying from 0.612 to 0.623. The corresponding CIE color coordinates ($x=0.273\sim0.276$, $y=0.325\sim0.330$ in white zone) are shown in Fig. 8 marked by ▲ and the inset presents the details of the chromaticity diagram, barely influenced by the doping concentration.

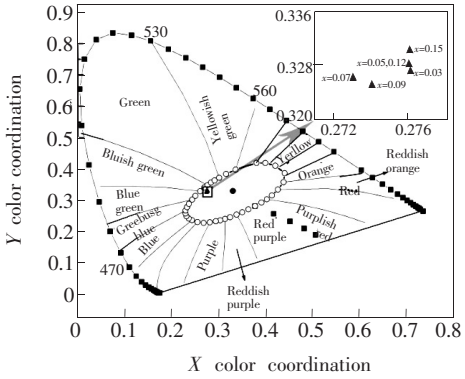

Fig. 8　The CIE color coordinates of α-$Ba_3Y_{1-x}(BO_3)_3$: xDy^{3+} ($\lambda_{ex}=350$ nm). The inset shows the details of the chromaticity diagram.

Distance between different Dy^{3+} ions decreases while increasing Dy^{3+} content and the non-radiative energy migration between different activators becomes more and more often, then the concentration quenching phenomenon occurs. The concentration quenching phenomenon usually origins from exchange interaction, dipole-dipole interaction, dipole-quadrupole interaction or quadrupole-quadrupole interaction. If the energy transfer occurs between same sort of activators, the strength of the multipolar interaction can be determined from the change in the emission intensity of the semi-stable state. According to Dexter's theory[24-25], the emission intensity (I) per activator ion follows equation (1):

$$\frac{I}{x}=\frac{k}{1+\beta(x)^{\theta/3}}, \tag{1}$$

where k and β are constants for the same excitation condition for a given host, x is the concentration of the activator, I is the emission intensity, and $\theta=3$, 6, 8 and 10 stands for exchange interaction, dipole-dipole interaction, dipole-quadrupole interaction and quadrupole-quadrupole interaction, respectively. The linear dependence of $\lg(I/x)$ on $\lg x$ is shown in the inset of Fig. 7 with an slope equaling −1.683 7. The value of θ is then calculated to be 5.051 1, close to 6, suggesting that dipole-dipole interaction is the main concentration quenching mechanism for Dy^{3+} in α-$Ba_3Y(BO_3)_3$ and the exchange interaction can not be ignored, either.

In the unit cell of α-$Ba_3Y(BO_3)_3$, Dy^{3+} ions tend to occupy Y sites in series of paralleled planes due to the same valence and similar ion radius (0.091 2 nm for Dy^{3+} and 0.090 0 nm for Y^{3+}). However, there are 6 nearest Ba3/Ba4 sites for every Y site with an distance between 0.382 3 and 0.393 9 nm, making the exchange of Ba^{2+} and Dy^{3+} (Y^{3+}) ions possible during the high temperature solid state reaction[18]. In other words, the following situation exists in this case: most Dy^{3+} ions take the Y sites forming Dy_I^{3+} luminescence center; others are exchanged with Ba^{2+} ions and located at Ba3/Ba4 sites forming Dy_{II}^{3+} center. The distance between these two luminescence centers, 0.387 6/0.390 9 nm, is short enough for exchange interaction, making θ less than 6.

3.4　Lifetime Decay Curves

To investigate the essential luminescence of Dy^{3+}, lifetime decay curves of α-$Ba_3Y_{1-x}(BO_3)_3$: xDy^{3+} are presented in Fig. 9 as well as fitting

results using the following second-order exponential function (2):

$$I = A_1\exp\left(-\frac{t}{\tau_1}\right) + A_2\exp\left(-\frac{t}{\tau_2}\right), \quad (2)$$

where A_1 and A_2 are constants, t is the time, τ_1 and τ_2 are rapid and slow decay lifetimes for exponential components, respectively. Further more, based on parameters A_1, A_2, τ_1 and τ_2 in equation (3), the average lifetime (τ^*) can be calculated by equation (3)[26]:

$$\tau^* = (A_1\tau_1^2 + A_2\tau_2^2)/(A_1\tau_1 + A_2\tau_2), \quad (3)$$

parameters τ_1, τ_2 and τ^* for decay curves of α-$Ba_3Y_{1-x}(BO_3)_3$:xDy^{3+} are demonstrated in Tab. 1. The average distance between two Dy^{3+} ions decreases with the increasing Dy^{3+} concentration, which enhances the energy migration or cross-relaxation between different Dy^{3+} ions *via* the dipole-dipole interaction or exchange interaction and decreases the luminescence lifetime from 0.808 ms to 0.360 ms[20,27-28]. The second-order exponential curves generate from the presence of two luminescence centers formed by Dy^{3+} taking both Y1/Y2 (CN:6) and Ba3/Ba4 sites (CN:9); the experimental behavior of α-$Ba_3Y_{1-x}(BO_3)_3$:xDy^{3+} can be ascribed to a linear superposition of Dy^{3+}_{I} and Dy^{3+}_{II}.

Tab. 1 The values of τ_1, τ_2 and τ^* for decay curves of α-$Ba_3Y_{1-x}(BO_3)_3$:xDy^{3+}.

x	τ_1/ms	τ_2/ms	τ^*/ms
0.03	0.303	1.07	0.808
0.05	0.267	0.987	0.951
0.07	0.222	0.874	0.845
0.09	0.152	0.638	0.508
0.12	0.115	0.444	0.382
0.15	0.095	0.421	0.360

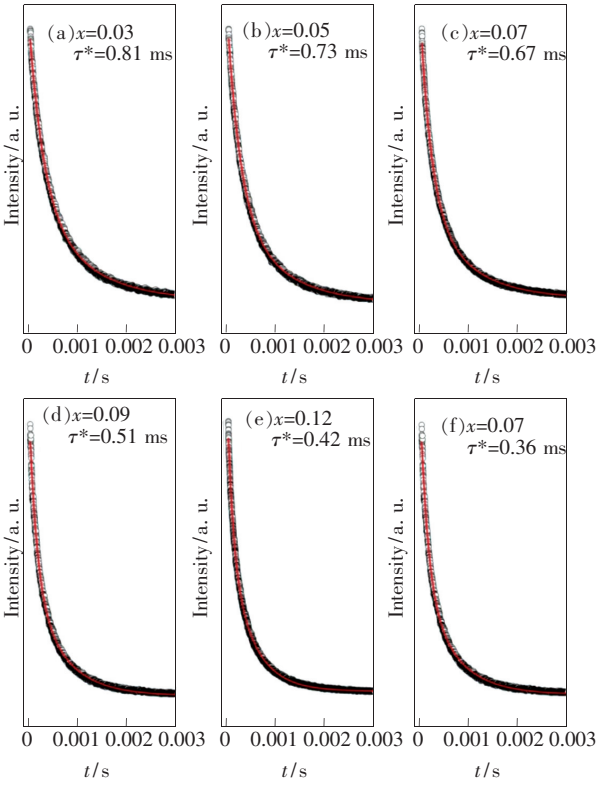

Fig. 9 Decay curves of α-$Ba_3Y_{1-x}(BO_3)_3$:xDy^{3+} (λ_{ex} = 350 nm, λ_{em} = 577 nm, room temperature, x = 0.03, 0.05, 0.07, 0.09, 0.12 and 0.15, respectively) and the corresponding fitting results (red lines)

4 Conclusion

A series of Dy^{3+} doped α-$Ba_3Y(BO_3)_3$ were synthesized by conventional solid state method at different temperature. The results indicate that phosphors synthesized at 1 100 ℃ have pure phase, most sufficient crystal growth and most intensive luminescence. Under 350 or 454 nm radiation, phosphors present white light emission with the CIE color coordinates around (0.273, 0.327), making the phosphor suitable for pc-WLEDs. The luminescence intensity is strongly influenced by Dy^{3+} concentration due to concentration quenching phenomenon. The concentration quenching mechanism and the second-order exponential decay curves are discussed in detail and supposed to be related to the specific unit cell structure of α-$Ba_3Y(BO_3)_3$.

Acknowledgements: This work was supported by Natural Science Foundation of Liaoning Province (20170540074).

References:

[1] SCHUBERT E F, KIM J K. Solid-state light sources getting smart [J]. *Science*, 2005, 308(5726):1274-1278.

[2] DUPUIS R D, KRAMES M R. History, development, and applications of high-brightness visible light-emitting diodes [J]. *J. Lightwave Technol.*, 2008, 26(9):1154-1171.

[3] ZHANG Y, GONG W J, YU J J, *et al.*. Tunable white-light emission *via* energy transfer in single-phase $LiGd(WO_4)_2$: Re^{3+} (*Re* = Tm, Tb, Dy, Eu) phosphors for UV-excited WLEDs [J]. *RSC Adv.*, 2015, 5(117):96272-96280.

[4] VAN DEUN R, NDAGSI D, LIU J, *et al.*. Dopant and excitation wavelength dependent color-tunable white light-emitting Ln^{3+}: Y_2WO_6 materials (Ln^{3+} = Sm, Eu, Tb, Dy) [J]. *Dalton Ttans.*, 2015, 44(33):5022-5030.

[5] WANG Y X, SONG Y H, ZHOU X Q, *et al.*. 3D-hierachical spherical $LuVO_4$: Tm^{3+}, Dy^{3+}, Eu^{3+}, microcrystal: synthesis, energy transfer, and tunable color [J]. *Chem. Eng. J.*, 2016, 306:155-163.

[6] CAO Y Y, LIU N D, TIAN J, *et al.*. Solid state synthesis and tunable luminescence of $LiSrPO_4$: Eu^{2+}/Mn^{2+}/Tb^{3+} phosphors [J]. *Polyhedron*, 2016, 107:78-82.

[7] DOBROWOLSKA A, KARSU E C, BOS A J J, *et al.*. Spectroscopy, thermoluminescence and afterglow studies of $CaLa_4(SiO_4)_3O$: *Ln* (*Ln* = Ce, Nd, Eu, Tb, Dy) [J]. *J. Lumin.*, 2015, 160:321-327.

[8] CHEN Y. J, CHEN L, XIAO L J, *et al.*. The effect of different lattice sites substitution on photoluminescence characteristics of Eu^{2+}/Ce^{3+} doped $M_5(ZO_4)_3X$ [J]. *Mat. Sci. Semicon. Proc.*, 2014, 18(1):59-64.

[9] SANG H J, KANG D S, JEON D Y. Effect of substitution of nitrogen ions to red-emitting $Sr_3B_2O_{6-3/2x}N_x$: Eu^{2+} *oxy*-nitride phosphor for the application to white LED [J]. *J. Cryst. Growth*, 2011, 326(1):116-119.

[10] LI P L, WANG Z J, YANG Z P, *et al.*. Luminescent characteristics of $LiCaBO_3$: *M* (*M* = Eu^{3+}, Sm^{3+}, Tb^{3+}, Ce^{3+}, Dy^{3+}) phosphor for white LED [J]. *J. Lumin.*, 2010, 130(2):222-225.

[11] DENAULT K A, CHENG Z Y, BRGOCH J, *et al.*. Structure-composition relationships and optical properties in cerium-substituted $(Sr,Ba)_3(Y,La)(BO_3)_3$ borate phosphors [J]. *J. Mater. Chem.* C, 2013, 1(44):7339-7345.

[12] AMAR N B, KOUBAA T, HASSAIRI M A, *et al.*. Optical spectroscopy of Eu^{3+} ions doped in $YAl_3(BO_3)_4$ crystal [J]. *J. Lumin.*, 2015, 160:95-100.

[13] HE J, SHI R, BRIK G M, *et al.*. Luminescence and multi-step energy transfer in $GdAl_3(BO_3)_4$ doped with Ce^{3+}/Tb^{3+} [J]. *J. Lumin.*, 2015, 161:257-263.

[14] CAI G M, SUN Y, LI H K, *et al.*. Crystal structure and photoluminescence of Tb^{3+}-activated $Ba_3InB_3O_9$ [J]. *Mater. Chem. Phys.* 2011, 129(3):761-768.

[15] ZHOU L Y, HUANG J L, YI L H, *et al.*. Luminescent properties of $Ba_3Gd(BO_3)_3$: Eu^{3+} phosphor for white LED applications [J]. *J. Rare Earth*, 2009, 27(1):54-57.

[16] CHUNG W K, JUNG H C, LEE C H, *et al.*. Warm with high color rendering index white light from hybridization of Ca_2BO_3Cl: Eu^{2+} yellow phosphor and CdSe/ZnS nanocrystals [J]. *J. Ind. Eng. Chem.*, 2013, 19(5):1743-1746.

[17] LI X X. Synthesis and luminescence properties of $Ba_3Y_{1-x}Eu_xB_3O_9$ ($0.05 \leqslant x \leqslant 0.35$) under UV excitation [J]. *Adv. Mater. Res.*, 2014, 906:60-65.

[18] CHENG Z Y, YU J J, ZHANG Y J, *et al.*. Luminescence and energy transfer mechanism of α-$Ba_3Y(BO_3)_3$: Ce^{3+}, Tb^{3+} [J]. *J. Lumin.*, 2017, 192:1004-1009.

[19] DURAIRAJAN A, BALAJI D, KAVI R K, *et al.*. Sol-gel synthesis and photoluminescence studies on colour tuneable Dy^{3+}/Tm^{3+} co-doped $NaGd(WO_4)_2$ phosphor for white light emission [J]. *J. Lumin.*, 2015, 157:357-364.

[20] MENG F G, ZHANG X M, SEO H J. Optical properties of Sm^{3+} and Dy^{3+} ions in $Gd_2MoB_2O_9$ host lattice [J]. *Opt. Laser Technol.*, 2012, 44(1):185-189.

[21] XU Q G, SUN J Y, CUI D P, *et al.*. Synthesis and luminescence properties of novel $Sr_3Gd(PO_4)_3$: Dy^{3+} phosphor [J]. *J. Lumin.*, 2015, 158:301-305.

[22] WANG D Y, CHEN T M, CHENG B M, *et al.*. Host sensitization of Tb^{3+} ions in tribarium lanthanide borates $Ba_3Ln(BO_3)_3$ (*Ln* = Lu and Gd) [J]. *Inorg. Chem.*, 2012, 51(51):2961-2965.

[23] JING L D, LIU X H, LI Y T, *et al.*. Synthesis and photoluminescence properties of $Ca_9Y(VO_4)_7$: Dy phosphors for white light-emitting diodes [J]. *J. Lumin.*, 2015, 162:185-190.

[24] DEXTER D L. A theory of sensitized luminescence in solids [J]. *J. Chem. Phys.*, 1953, 21(5):836-850.

[25] VAN UITERT L G. Characterization of energy transfer interactions between rare earth ions [J]. *J. Electrochem. Soc.*, 1967, 114(10):1048-1053.

[26] WANG L X, XU M J, ZHAO H Y, *et al.*. Luminescence, energy transfer and tunable color of Ce^{3+}, Dy^{3+}/Tb^{3+} doped

$BaZn_2(PO_4)_2$ phosphors [J]. *New J. Chem.*, 2016, 40(4):3086-3093.

[27] WU X, HUANG Y L, SHI L, *et al.*. Spectroscopy characteristics of vanadate $Ca_9Dy(VO_4)_7$, for application of white-light-emitting diodes [J]. *Mater. Chem. Phys.*, 2009, 116(2-3):449-452.

[28] ZHANG Z W, SONG A J, YUE Y, *et al.*. White light emission from $Ca_9Bi(PO_4)_7:Dy^{3+}$, single-phase phosphors for light-emitting diodes [J]. *J. Alloys Compd.*, 2015, 650(47):410-414.

宁宏宇(1994 -),女,辽宁丹东人,硕士研究生,2017 年于大连工业大学获得学士学位,主要从事白光 LED 荧光粉的研究。

E-mail: 873764576@qq.com

张彦杰(1981 -),男,山西祁县人,博士,副教授,2008 年于中国科学院兰州化学物理研究所获得博士学位,主要从事白光 LED 用新型高效发光材料的研究。

E-mail: zhang_yj@dlpu.edu.cn

于晶杰(1974 -),女,辽宁大连人,博士,教授,2013 年于大连理工大学获得博士学位,主要从事半导体照明发光材料以及光源器件的研究。

E-mail: yujingjie@dlpu.edu.cn